

Article

Seasonal Variations in the Flow of Land-Terminating Glaciers in Central-West Greenland Using Sentinel-1 Imagery

Adriano Lemos * , Andrew Shepherd, Malcolm McMillan and Anna E. Hogg

Centre for Polar Observation and Modelling, University of Leeds, Leeds LS2 9JT, UK;
A.Shepherd@leeds.ac.uk (A.S.); M.McMillan@leeds.ac.uk (M.M.); A.E.Hogg@leeds.ac.uk (A.E.H.)

* Correspondence: A.G.Lemos14@leeds.ac.uk

Received: 6 October 2018; Accepted: 21 November 2018; Published: 24 November 2018



Abstract: Land-terminating sectors of the Greenland ice sheet flow faster in summer after surface meltwater reaches the subglacial drainage system. Speedup occurs when the subglacial drainage system becomes saturated, leading to a reduction in the effective pressure which promotes sliding of the overlying ice. Here, we use observations acquired by the Sentinel-1a and b synthetic aperture radar to track changes in the speed of land-terminating glaciers across a 14,000 km² sector of west-central Greenland on a weekly basis in 2016 and 2017. The fine spatial and temporal sampling of the satellite data allows us to map the speed of summer and winter across the entire sector and to resolve the weekly evolution of ice flow across the downstream portions of five glaciers. Near to the ice sheet margin (at 650 m.a.s.l.), glacier speedup begins around day 130, persisting for around 90 days, and then peaks around day 150. At four of the five glaciers included in our survey the peak speedup is similar in both years, in Russell Glacier there is marked interannual variability of 32% between 2016 and 2017. We present, for the first time, seasonal and altitudinal variation in speedup persistence. Our study demonstrates the value of Sentinel-1's systematic and frequent acquisition plan for studying seasonal changes in ice sheet flow.

Keywords: Sentinel-1; ice velocity; land-terminating glacier; Synthetic Aperture Radar; Greenland

1. Introduction

In recent decades the Greenland Ice Sheet has lost ice at an increasing rate, rising by 89% between 2011–2014 relative to 1992–2011 [1,2]. The majority (60%) of this ice loss has been due to surface melting and runoff [3,4], which have risen as summers have warmed [5,6]. Between 2011 and 2014, 41% of all ice loss from Greenland (269 ± 51 GT yr⁻¹; [2]) was from the south-western sector alone, where changes in the degree of surface melting have been pronounced [7].

In addition to the direct impact on runoff, increased surface melting has also been linked to increases in the speed of ice flow through basal lubrication [8–10]. Rising air temperatures lead to increased surface melting, which can in turn lead to an increase in the amount of water feeding into the subglacial drainage system [10] after supraglacial lakes drain or moulins open [9,10]. As a consequence of this excess meltwater, subglacial water pressure rises, which reduces the effective pressure between the ice-bedrock interface and leads to enhanced basal sliding [11–13]. During the melting season, frictional heating caused by water flow enlarges the conduits of the subglacial hydrologic system, allowing a greater volume of water to be accommodated [14,15]. As a consequence, from mid-season to the end of the melt season, the drainage system transmission capacity exceeds the meltwater input, draining water efficiently through low-pressure channels [15,16].

Seasonal changes in ice flow have been observed in both fast-moving and slow-moving glaciers [17–23]. In south-west Greenland, the summertime speedup of land-terminating glaciers

is widespread and is widely interpreted as being driven by seasonal changes in the degree of basal lubrication [8,20,24]. At low elevations (under 1000 m), seasonal changes in the movement of Greenland's glaciers are thought to be dominated by short-term events, typically lasting between 1 day to 1 week during the summer [25,26], with ice speeds increasing by 100% to 150% relative to winter [20,27]. Resolving such changes has been a challenge, because observations of ice sheet flow have historically been made using episodically acquired satellite imagery [7,11,12] and GPS sensors installed at point locations on the ice sheet [14,19,25]. Systematically monitoring seasonal variations in ice flow is therefore an important task as it will improve our understanding of the present and likely future response of the Greenland Ice Sheet to a changing climate.

Since the 1970s, the speed of glacier flow in the polar regions has been measured with repeat optical satellite imagery [28]. However, despite their ongoing use [29–32], optical images are daylight dependent which limits their utility outside of the summer season. Unfortunately, satellite imagery may also be obscured by clouds. Synthetic aperture radar (SAR) images do not suffer from either limitation and have also been extensively used to measure ice speed since the launch of the European Remote Sensing Satellite 1 (ERS-1) in 1991 [33–37]. A persistent obstacle to the use of both optical and SAR satellite imagery for tracking ice motion has been the episodic nature of acquisitions. Since the launch of the Sentinel-1a (S1a) and Sentinel-1b (S1b) SAR constellation in April 2014 and April 2016, respectively, it has become possible to systematically measure changes in ice speed every 6 days [38–40]. Here, we use a sequence of Sentinel-1a and 1b SAR images to track seasonal changes in ice sheet flow across a land-terminating sector of the Greenland Ice Sheet between 2014 and 2017.

2. Study Area

Our study focusses on a 14,000 km² sector of central-west Greenland between 66.6°N–67.4°N (Figure 1). The study area includes five glaciers; Isorlersuup Glacier (IG), Ørkendalen Glacier (ØG), Russell Glacier (RG) and Isunnguata Sermia (IS), and an unnamed outlet glacier which we refer to as Glacier 1 (G1). The area has received a relatively high amount attention due to the propensity of its glaciers to exhibit seasonal speedup. In-situ GPS observations have shown that seasonal velocity variations are strongly linked to changes in surface melting [14,19,25,26,41–43]. Satellite measurements have provided a large-scale perspective of changes in ice flow [18,20,21,27] and in the extent of supraglacial lakes [44–47]. Together, these measurements, in conjunction with numerical ice flow modelling have led to an improved understanding of the link between regional hydrology and changes in ice flow, for example the role of supra-glacial lake drainage [48,49].

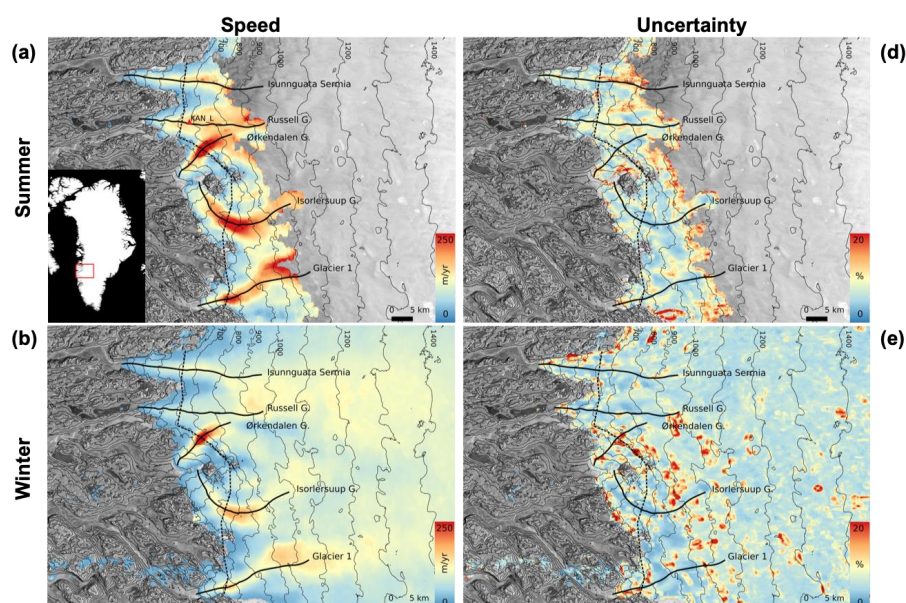


Figure 1. Cont.

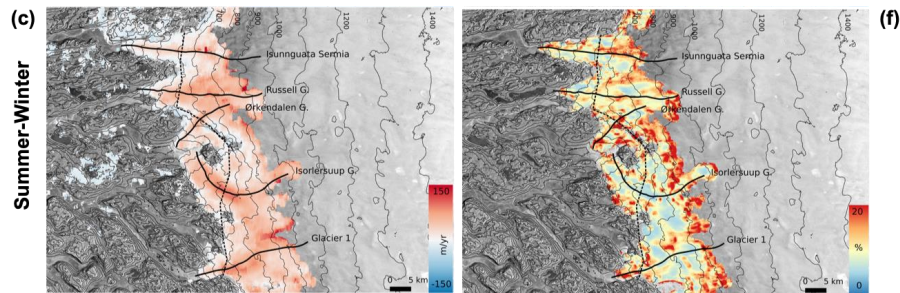


Figure 1. Average ice velocity in (a) summer (May–Jul), (b) winter (Aug–Apr), and (c) the difference between summer and winter, derived from Sentinel-1 (S1) synthetic aperture radar (SAR) imagery. The uncertainties in the maps associated with the summer, winter, and difference between the summer and winter ice speeds are also shown (d–f, respectively). Velocities and the uncertainties are overlaid on a SAR backscatter intensity image. Also shown are elevation contours (thin grey lines), profiles along (solid black lines) and across (dotted black lines) the centre of five glaciers. The location of the KAN_L weather station is also mapped (red dot, a).

3. Data and Methods

Previous studies have demonstrated the capability of Sentinel-1 (S1) for mapping ice sheet flow [38–40]. Here, we use single-look complex (SLC) synthetic aperture radar (SAR) images acquired in the interferometric wide (IW) mode to investigate the detailed patterns of seasonal glacier velocity change. The images used were acquired between January 2016 and December 2017, with a revisit time of 6 or 12 days due to the repeat cycle of 12 days and the 180 degree orbital phase difference between the two satellites. We used the GAMMA-SAR software [50] to generate 96 individual ice velocity maps from different pairs of Sentinel-1a (S1a) and Sentinel-1b (S1b) SAR images.

Ice velocities were computed using a feature tracking technique applied to SAR backscatter intensity images [51], assuming that the ice flow occurs parallel to the surface and at a constant rate during the image acquisition period. This is a well-established technique, measuring the displacement of similar SAR image features (e.g., crevasses and speckle patterns) based on a cross correlation algorithm applied to image segments (windows) in two co-registered SAR images [40,51–53]. The window and step size used was based on sensitivity testing of a range of values, where a trade-off between the spatial resolution, spatial coverage and measurement accuracy of the output result were considered. For an individual pair, the end results depend on the change in snow surface properties between the processed images, the correlation of the speckle pattern, and the scale of the local features observed. For the present study, ice motion was estimated using window sizes of 350×75 pixels in ground range and azimuth, respectively, corresponding to dimensions of approximately 1.7 and 1.5 km. We used the Greenland Ice Mapping Project (GIMP) digital elevation model (DEM) [54] to geocode the displacements, and the final velocity measurements were posted on to a regular 100 m grid. The post-processing to remove poor quality data followed the methodology of Lemos et al. [40]. We applied a low-pass filter twice, using a kernel of 1 km by 1 km, rejecting values where the deviation between the unfiltered and filtered speed magnitude exceeded 30%. Finally, we apply a labelling algorithm based on the image histogram, identifying regions with similar values and rejecting non-coherent velocity magnitudes and isolated measurements with an area smaller than 1/1000th of the processed image size.

Errors in ice velocity measurements derived from repeat satellite imagery can be caused by inaccurate image co-registration, mis-modelled terrain correction [38,55] and atmospheric interference, including changes in ionospheric properties and in tropospheric water vapour [56]. To estimate velocity errors, we scale each individual velocity map by the time-averaged signal to noise ratio (SNR) of the cross-correlation function [40]. The SNR is determined as the ratio between the cross-correlation function peak (C_p) and the average correlation level (C_l) on the tracking window used to estimate the

velocities [57]. Typically, the estimated velocity error is ~10% across the majority of the study area, rising to 20% in regions lacking stable features (Figure 1d–f).

4. Results and Discussion

First, we generated average summer and winter regional velocity maps (Figure 1a,b, respectively) in each calendar year using images that fell within the average periods of the start and end days of speedup in the sector (Table 1). The velocity coverage is better in winter than summer, especially over the slow-moving inland ice, due to the absence of melting. During winter, the scattering properties of the snowpack are relatively stable and this allows radar speckle to be tracked over the otherwise featureless terrain [51,53]. In contrast, the retrieval of summer velocities is limited to within ~30 km of the ice sheet margin where there is a sufficient amount of persistent physical features to be able to track motion. Nevertheless, because of the relatively large number of individual velocity maps, we were able to resolve the seasonal pattern of speedup with unprecedented detail and show, for example, that speedup is clearly concentrated towards the centre of each glacier (Figure 1c).

Table 1. Seasonal velocity, speedup, speedup persistence, ice thickness and surface slope of the five glaciers averaged in two elevations bands (P1, between 650 and 750 m.a.s.l.; P2, over 820 m.a.s.l.).

Location		Summer Speed (m yr ⁻¹)	Winter Speed (m yr ⁻¹)	Speedup Relative to Winter (%)	Summer Velocity Peak (m yr ⁻¹)	Annual Mean Velocity (m yr ⁻¹)	Speedup Start Day	Speedup End Day	Speedup Persistence (days)	Mean Thickness (m)	Mean Slope (%)
Glacier 1	P1	187 ± 13	125 ± 9	49%	214 ± 13	133 ± 10	136	196	60	470	2.2%
	P2	154 ± 18	109 ± 10	41%	176 ± 18	116 ± 11	153	216	63	650	2.0%
Isorlersuup	P1	220 ± 11	156 ± 8	41%	257 ± 11	166 ± 9	134	209	75	516	2.2%
	P2	148 ± 17	119 ± 10	24%	169 ± 17	124 ± 11	143	212	69	612	1.6%
Ørkendalen	P1	246 ± 16	203 ± 22	21%	259 ± 16	212 ± 22	113	198	85	390	2.8%
	P2	163 ± 17	111 ± 9	47%	205 ± 17	118 ± 11	155	212	57	623	1.5%
Russell G.	P1	121 ± 13	87 ± 5	38%	139 ± 13	93 ± 7	137	211	74	559	2.2%
	P2	156 ± 18	113 ± 10	38%	177 ± 18	118 ± 11	160	215	55	692	1.9%
Isunguata S.	P1	103 ± 9	93 ± 6	11%	112 ± 9	95 ± 7	136	201	64	615	2.1%
	P2	121 ± 21	79 ± 5	53%	145 ± 21	87 ± 7	178	250	71	802	1.5%
Sector	P1	175 ± 28	132 ± 26	32%	196 ± 28	140 ± 28	131	203	72	510	2.3%
	P2	148 ± 41	106 ± 20	40%	174 ± 41	113 ± 23	158	221	63	676	1.7%

The maximum recorded winter speed ranges from 121 ± 5 m yr⁻¹ at IS to 296 ± 22 m yr⁻¹ at ØG, and the maximum recorded summer speed ranges from 196 ± 18 m yr⁻¹ at RG to 359 ± 18 m yr⁻¹ at ØG. In general, the degree of speedup at each glacier is quite variable, in agreement with the findings of a previous survey based on TerraSAR-X measurements acquired in 2009 and 2010 in the same region [27]. Locally, we observe numerous regions where the seasonal speedup is greater than 100 m yr⁻¹, for instance reaching 150 m yr⁻¹ (~75%) near to the glacier fronts of IG and RG (Figure 1c). Our results agree well with previous studies in the same region. For example, seasonal velocity changes of 50–100% between 2004 and 2007 have been reported [18], and Sundal et al. [20] reported speedup in the range of 50–125% between 1993 and 1998. Not all glaciers, however, show such a large degree of speedup. The neighbouring glacier ØG, for example, exhibits a much lower seasonal speedup of ~30 m yr⁻¹ (21%), and maintains relatively high rates of ice flow even during winter months near the ice margin.

We examined the geometrical configurations of each glacier to investigate the possible reasons for the heterogeneous speedup (Figure 2) using surface and bed elevations from GIMP-DEM [54] and IceBridge BedMachine Greenland, Version 3 [58], respectively. Although the surface slopes of the glaciers are relatively uniform (2.8% at ØG and 2% elsewhere), their average thicknesses are considerably more variable (from 390 m at ØG to 802 m at IS). The five glaciers also present different flow regimes and, in contrast to marine-terminating glaciers [34,35], reach their peak speeds at distances between 8 and 18 km inland. At G1, IG and ØG, this location is approximately 650 m.a.s.l. The relative speedup is non-uniform and excluding IS where the velocity profile is incomplete, ranges from 21 to 49% (Table 1). Despite being the fastest glacier, ØG had the lowest seasonal variation of all the studied glaciers (Table 1), which suggests that its flow was predominantly driven either by gravity with a low

sensitivity to transient increases in basal lubrication, or it had been influenced by non-uniform basal motion due to friction at the bed-ice interface [59,60].

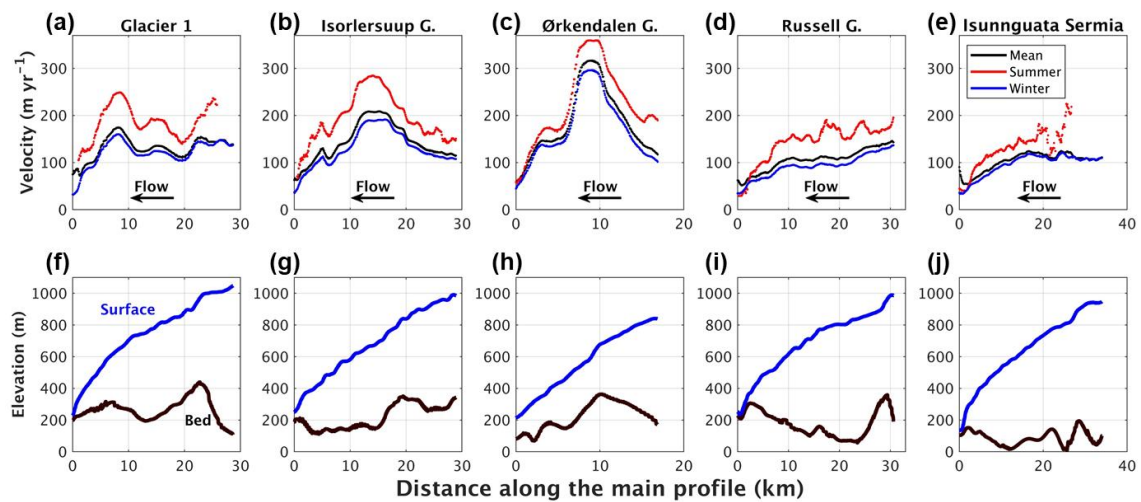


Figure 2. Mean summer and winter ice velocity (a–e) and geometry (f–j) along central profiles of five glaciers in west-central Greenland (see Figure 1 for glacier locations) in 2016 and 2017. Surface and bed elevations are from the Greenland Ice Mapping Project digital elevation model (GIMP-DEM) [54] and IceBridge BedMachine Greenland, Version 3 [58], respectively.

Our velocity maps have sufficient spatial coverage to provide continuous profiles of summer and winter ice speed across the central flow unit of each glacier (Figure 3). Speedup is primarily confined to the central, fast flowing parts of each glacier and at ~600 m.a.s.l., peaks in the range of 22% (ØG) to 66% (RG). At this altitude all of the glaciers sit in distinct bedrock depressions where the ice is far thicker than in the slower flowing neighbouring regions. In general, speedup is largely confined to fast-flowing glaciers or their tributaries (e.g., at 25–30 km and 58–60 km along the transect). Local variations in the input and routing of surface melt water may be responsible for this heterogeneity in the degree of seasonal ice speedup. With the exception of RG, the regional glaciers do not show inter-annual variations in the degree of summer speedup. At RG, however, summer rates of ice flow were 32% faster in 2016 than in 2017. This indicates that changes in a single glacier system are not always indicative of wider patterns, highlighting the value of large-scale systematic satellite monitoring. The only other place of significant inter-annual difference in seasonal speedup is the slow flowing sector between RG and IS. Here, however, ice flowed faster in 2017 than in 2016.

A unique benefit of the S1 constellation is its systematic and high temporal sampling, which supports continuous, multi-year records of ice motion. For each of the glaciers in our study region, we explored this novel capability by charting their speed every 6 days across two full seasonal cycles (Figure 4). We then analysed the velocity time-series within two distinct elevation bands: 650–750 m.a.s.l. (P1) and above 820 m.a.s.l. (P2) to investigate differences in their seasonal flow at high and low altitudes (Table 1). There is clear heterogeneity in the seasonal flow of the five principal glaciers in this sector of the ice sheet (Figure 4). G1, IG and RG exhibited coherent speedup periods during summer time at both altitudes. ØG showed a clear seasonal cycle at high elevations, but at lower elevations the seasonality was much less pronounced and is characterized by a longer duration speedup over the winter months, and at IS there was no apparent summer speedup at either location. However, the velocity data in these regions is generally of poorer quality than elsewhere due to the absence of clear persistent features in the SAR imagery, limiting our ability to draw firm conclusions about seasonal changes in ice flow in these glaciers. At the three glaciers where a coherent seasonal cycle is resolved, in all cases our data show that lower elevations (P1) speed up first, followed by the upper elevations (P2).

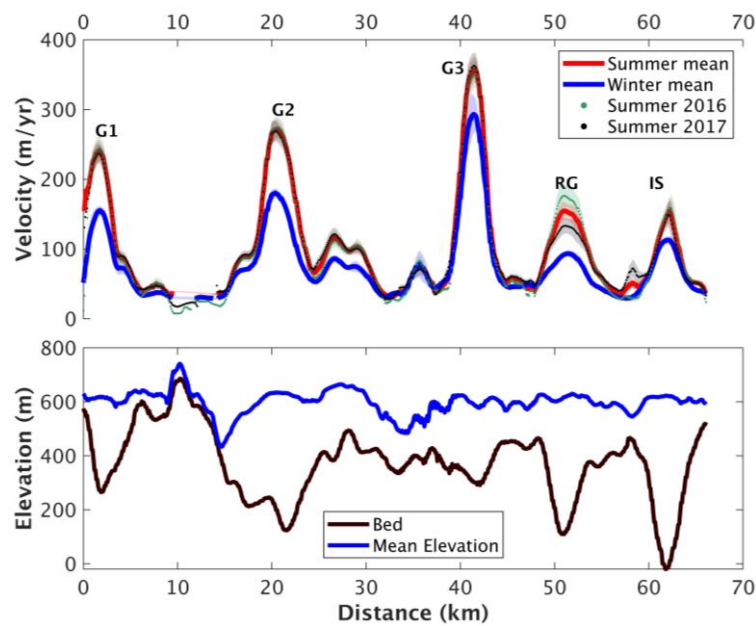


Figure 3. Ice velocity (Top), with uncertainty ranges represented by the light shading, and geometry (Bottom) along an across-flow profile of the study area (see Figure 1 for location) in 2016 to 2017.

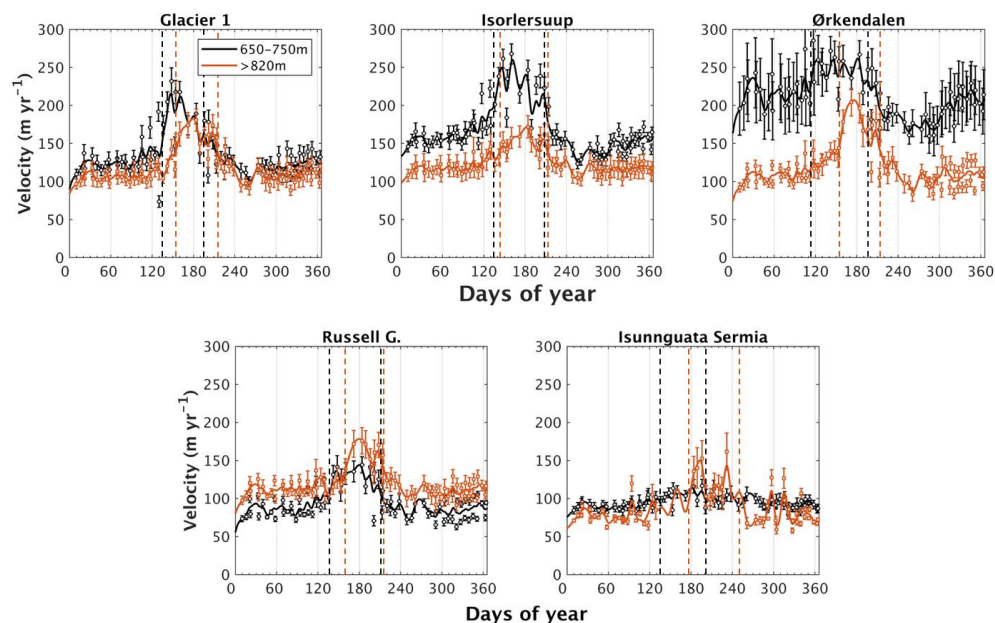


Figure 4. Seasonal changes in ice flow at two different elevation bands on each glacier. Actual measurements are represented by the dots, spline fits as continuous lines, and speedup periods the intervals between the consecutive coloured dotted lines.

We analysed the velocity data to determine the persistence of speedup, and the start and end day of the summer season across the sector. To do this, we first applied a spline fit to each velocity time-series and identified local maxima using the precompiled MATLAB function ‘findpeaks’. We then identified the peak speedup, rejecting locations under a prominent peak threshold of 25 m yr^{-1} . After testing thresholds of 25, 50 and 70 m yr^{-1} we found that this threshold provided a reasonable balance between spatial coverage and consistent speedup persistence, even in slow-moving areas. We also found the number of prominent peaks per pixel which are on average between 1 and 3, as well as consistent speedup persistence results. The persistence of the summer season is defined by the duration of the width of the peak, shown as the time interval between the dotted lines in Figure 4.

For time-series which exhibit multiple and consecutive prominent peaks, we calculate the speedup persistence as the sum of each peak width. However, when this occurs, we calculate the start and end dates of the summer season using the first and last prominent peaks, respectively (Figure 5b,c). We applied the method to spatially-averaged time-series within discrete elevation bands (P1 and P2, Figure 4) and also at individual locations to resolve the spatial pattern (Figure 5).

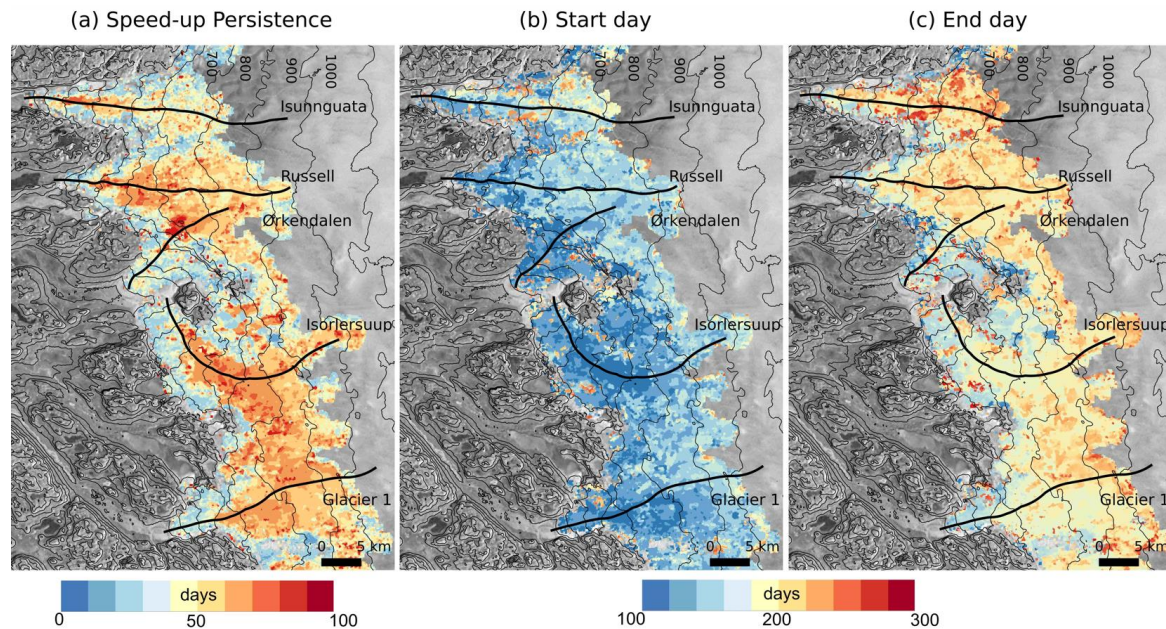


Figure 5. Persistence of ice speedup (a), the start (b) and end date (c) of the summer season.

Across all glaciers, the persistence of seasonal speedup ranges from 72 to 63 days at P1 and P2, respectively (Table 1). The persistence of speedup is shorter at higher elevations on all glaciers except G1. At RG, our estimated persistence of 55 days at P2 is lower but similar to the 66 day estimate made by Palmer et al. [21] for the period of 2004–2007 at the same location. For the first time we are able to map spatial variations in the pattern of summer speedup persistence (Figure 5). The persistence of summer speedup shows clear altitudinal variation at all glaciers, ranging from 60 to 90 days and from 50 to 70 days, respectively, at P1 and P2. At IG, speedup generally has a duration of around 75 days, but persists for 80 days at isolated locations in the fastest flowing section of the glaciers (around 700 m.a.s.l.). In general, at lower altitudes (<500 m.a.s.l.), speedup persists for a significantly shorter period (~40 days). Lower regions are likely to have relatively high surface melting, potentially supplying more water to the subglacial drainage system, allowing channels to develop sooner and thereby shortening the speedup period [15,16]. We estimated the start and end dates of the summer season using the date of peak speedup and the persistence, assuming the period is symmetrical. Near to the ice sheet margin (P1), summertime speedup begins around day 130 and lasts for around 90 days (Table 1 and Figure 5). The summer duration affects a wider section of the ice sheet up to 25 km inland, however the onset date is delayed by approximately 25 days on average at higher elevations (P2).

To investigate the relationship between seasonal velocity changes and environmental forcing in more detail, we compared the regional variation to a local estimate of surface melting. For this comparison, we computed the mean velocity of G1, IG and RG in 2017, when a continuous 6-day sampling was possible (Figure 6). ØG and IS were excluded due to their unusual geometry (high slope) and relatively poor tracking coverage, respectively. We then computed positive degree days (PDDs) as a measure of the surface melting (Figure 6) using air temperatures recorded at the nearby KAN_L (670 m.a.s.l., Figure 1a) automatic weather station and distributed by the Programme for Monitoring of the Greenland Ice Sheet (PROMICE, <https://www.promice.dk/WeatherStations.html>). PDD's were integrated over six day periods to match the sampling of the satellite velocity measurements.

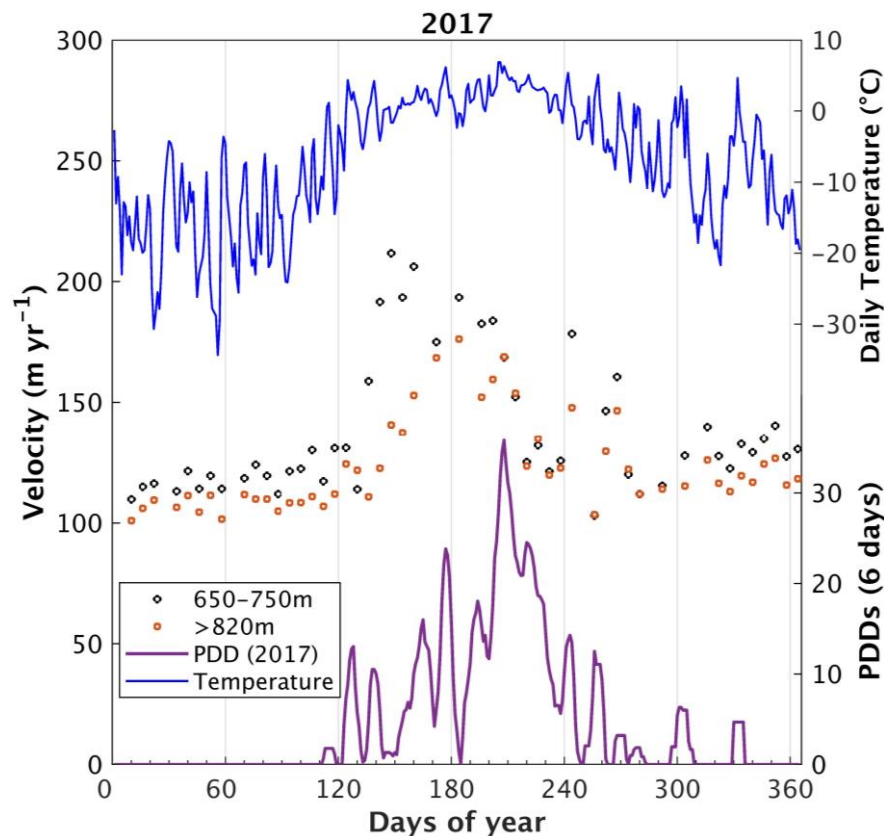


Figure 6. Averaged speed of three glaciers (G1, IG, and RG) with similar geometry and data sampling at two elevations bands during 2017. Also shown are daily temperature and positive degree days (PDDs) recorded at the nearby KAN_L automatic weather station (670 m.a.s.l.) and distributed by the Programme for Monitoring of the Greenland Ice Sheet.

The onset of speedup begins shortly after the first PDDs was recorded at KAN_L on day 125. Onset began on day 130 at P1 and on day 140 at P2. The high speeds were sustained for ~ 90 days at P1 and ~ 80 days at P2. The seasonal speedup, likely caused by melt-induced acceleration [8,14,61], starts in P1 shortly after the melt onset possibly reaches the bed (e.g., through moulins or crevasses), followed by P2, located at higher elevation and then undergoing less melting [10,14,18,23]. Future investigations using the SAR backscatter information will improve the characterization of the surface melt days. After the maximum PDDs were reached on day 207, the ice speed at P1 and P2 began to slow down rapidly at similar rates, returning to near winter levels by day 220. Two further speedup events then occur around days 244 and 268 and these coincide with isolated short-lived melt events evident within the PDD record. Later spikes in velocity, enhanced by short-term basal sliding, are likely to happen due to excess amount of water input combined with the time required for the drainage system to accommodate the extra melt-water, since the size of cavities adjusts progressively in time [14,16].

5. Conclusions

We have computed seasonal changes in the motion of five land-terminating glaciers in the central-west sector of the Greenland Ice Sheet using Sentinel-1a and-1b synthetic aperture radar imagery. The systematic acquisition schedule of Sentinel-1 provides a capacity to track ice motion with significantly greater spatial and temporal sampling than previous satellite missions. In our study, we were able to produce 96 unique ice velocity maps over a two-year period, which corresponds to approximately four times the sampling frequency of previous studies [20,21,27]. The high data volumes allow us to study spatial and temporal changes in ice flow across this sector of the Greenland ice sheet. Despite being located in the same sector and being exposed to similar environmental

conditions, the five glaciers we have surveyed show different patterns of speedup; peak summer speedup for example ranges from 21% (Ørkendalen) to 49% (Glacier 1) relative to winter. Speedup is clearly concentrated along the central portions of each glacier, with only isolated instances elsewhere. For the first time we mapped spatial variations in the seasonal speedup persistence cycle. In this sector, the start date of the speedup period ranges from day 113 to 178, and the end date ranges from day 196 to 250, leading to a persistence ranging from 55 to 85 days. Our study highlights the unique value of the Sentinel-1 mission for tracking short term changes in ice motion.

Author Contributions: A.L. led the project and wrote the paper, supervised by A.S., M.M. and A.E.H. A.L. and A.E.H. processed the data. All authors discussed the results and commented on the manuscript at all stages.

Funding: This work was led by the NERC Centre for Polar Observation and Modelling, supported by the Natural Environment Research Council (cpom300001), with the support of a grant (4000107503/13/I-BG), and the European Space Agency. Adriano Lemos was supported by the CAPES-Brazil PhD scholarship. Anna E. Hogg is funded by the European Space Agency's support of Science Element program and an independent research fellowship (4000112797/15/I-SBo).

Acknowledgments: The authors gratefully acknowledge the European Space Agency for the Copernicus Sentinel 1 data acquired from Data Hub, courtesy of the EU/ESA. The Sentinel-1 data are freely available at <https://scihub.copernicus.eu/> (last access: 18 September 2018). Data from the Programme for Monitoring of the Greenland Ice Sheet (PROMICE) and the Greenland Analogue Project (GAP) were provided by the Geological Survey of Denmark and Greenland (GEUS) at <http://www.promice.dk>. This work was led by the NERC Centre for Polar Observation and Modelling, supported by the Natural Environment Research Council (cpom300001), with the support of a grant (4000107503/13/I-BG), and the European Space Agency. Anna E. Hogg is funded by the European Space Agency's support of Science Element program and an independent research fellowship (4000112797/15/I-SBo). Adriano Lemos was supported by the CAPES-Brazil PhD scholarship. We thank the editor Suzanne Ji, and the four reviewers for their comments, which helped to improve the manuscript.

Conflicts of Interest: The authors declare no conflict of interest.

References

1. Shepherd, A.; Ivins, E.R.; Geruo, A.; Barletta, V.R.; Bentley, M.J.; Bettadpur, S.; Briggs, K.H.; Bromwich, D.H.; Forsberg, R.; Galin, N.; et al. A Reconciled Estimate of Ice-Sheet Mass Balance. *Science* **2012**, *338*, 1183–1189. [[CrossRef](#)] [[PubMed](#)]
2. McMillan, M.; Leeson, A.; Shepherd, A.; Briggs, K.; Armitage, T.W.K.; Hogg, A.; Munneke, P.K.; van den Broeke, M.; Noël, B.; Berg, W.J.; et al. A high resolution record of Greenland mass balance. *Geophys. Res. Lett.* **2016**, *43*, 1–9. [[CrossRef](#)]
3. Enderlin, E.M.; Howat, I.M.; Jeong, S.; Noh, M.-J.; van Angelen, J.H.; van den Broeke, M.R. An improved mass budget for the Greenland ice sheet. *Geophys. Res. Lett.* **2014**, *41*, 1–7. [[CrossRef](#)]
4. Van den Broeke, M.; Enderlin, E.; Howat, I.; Kuipers Munneke, P.; Noël, B.; van de Berg, W.J.; van Meijgaard, E.; Wouters, B. On the recent contribution of the Greenland ice sheet to sea level change. *Cryosphere* **2016**, *10*, 1933–1946. [[CrossRef](#)]
5. Hanna, E.; Mernild, S.H.; Cappelen, J.; Steffen, K. Recent warming in Greenland in a long-term instrumental (1881–2012) climatic context: I. Evaluation of surface air temperature records. *Environ. Res. Lett.* **2012**, *7*. [[CrossRef](#)]
6. Hanna, E.; Fettweis, X.; Mernild, S.H.; Cappelen, J.; Ribergaard, M.H.; Shuman, C.A.; Steffen, K.; Wood, L.; Mote, T.L. Atmospheric and oceanic climate forcing of the exceptional Greenland ice sheet surface melt in summer 2012. *Int. J. Climatol.* **2014**, *34*, 1022–1037. [[CrossRef](#)]
7. Crozier, J.; Karlstrom, L.; Yang, K. Basal control of supraglacial meltwater catchments on the Greenland Ice Sheet. *Cryosphere* **2018**, *12*, 3383–3407. [[CrossRef](#)]
8. Zwally, H.J.; Abdalati, W.; Herring, T.; Larson, K.; Saba, J.; Steffen, K. Surface Melt—Induced Acceleration of Greenland Ice-Sheet Flow. *Science* **2002**, *297*, 218–223. [[CrossRef](#)] [[PubMed](#)]
9. Hoffman, M.J.; Catania, G.A.; Neumann, T.A.; Andrews, L.C.; Rumrill, J.A. Links between acceleration, melting, and supraglacial lake drainage of the western Greenland Ice Sheet. *J. Geophys. Res. Earth Surf.* **2011**, *116*, 1–16. [[CrossRef](#)]
10. Chu, V.W. Greenland ice sheet hydrology: A review. *Prog. Phys. Geogr.* **2014**, *38*, 19–54. [[CrossRef](#)]

11. Harper, J.T.; Humphrey, N.F.; Pfeffer, W.T.; Fudge, T.; O'Neel, S. Evolution of subglacial water pressure along a glacier's length. *Ann. Glaciol.* **2005**, *40*, 31–36. [[CrossRef](#)]
12. Nienow, P.W.; Hubbard, A.L.; Hubbard, B.P.; Chandler, D.M.; Mair, D.W.F.; Sharp, M.J.; Willis, I.C. Hydrological controls on diurnal ice flow variability in valley glaciers. *J. Geophys. Res. Earth Surf.* **2005**, *110*, 1–11. [[CrossRef](#)]
13. Andrews, L.C.; Catania, G.A.; Hoffman, M.J.; Gulley, J.D.; Lüthi, M.P.; Ryser, C.; Hawley, R.L.; Neumann, T.A. Direct observations of evolving subglacial drainage beneath the Greenland Ice Sheet. *Nature* **2015**, *514*, 80–83. [[CrossRef](#)] [[PubMed](#)]
14. Bartholomew, I.D.; Nienow, P.; Mair, D.; Hubbard, A.; King, M.A.; Sole, A. Seasonal evolution of subglacial drainage and acceleration in a Greenland outlet glacier. *Nat. Geosci.* **2010**, *3*, 408–411. [[CrossRef](#)]
15. Cowton, T.; Nienow, P.; Sole, A.; Wadhwa, J.; Lis, G.; Bartholomew, I.D.; Mair, D.; Chandler, D. Evolution of drainage system morphology at a land-terminating Greenlandic outlet glacier. *J. Geophys. Res. Earth Surf.* **2013**, *118*, 29–41. [[CrossRef](#)]
16. Schoof, C. Ice-sheet acceleration driven by melt supply variability. *Nature* **2010**, *468*, 803–806. [[CrossRef](#)] [[PubMed](#)]
17. Rignot, E.; Kanagaratnam, P. Changes in the Velocity Structure of the Greenland Ice Sheet. *Science* **2006**, *311*, 986–990. [[CrossRef](#)] [[PubMed](#)]
18. Joughin, I.; Das, S.B.; King, M.A.; Smith, B.E.; Howat, I.M.; Moon, T. Seasonal Speedup along the Western Flank of the Greenland Ice Sheet. *Science* **2008**, *320*, 781–784. [[CrossRef](#)] [[PubMed](#)]
19. Shepherd, A.; Hubbard, A.; Nienow, P.; King, M.; McMillan, M.; Joughin, I. Greenland ice sheet motion coupled with daily melting in late summer. *Geophys. Res. Lett.* **2009**, *36*, 1–4. [[CrossRef](#)]
20. Sundal, A.V.; Shepherd, A.; Nienow, P.; Hanna, E.; Palmer, S.; Huybrechts, P. Melt-induced speed-up of Greenland ice sheet offset by efficient subglacial drainage. *Nature* **2011**, *469*, 521–524. [[CrossRef](#)] [[PubMed](#)]
21. Palmer, S.; Shepherd, A.; Nienow, P.; Joughin, I. Seasonal speedup of the Greenland Ice Sheet linked to routing of surface water. *Earth Planet. Sci. Lett.* **2011**, *302*, 423–428. [[CrossRef](#)]
22. Joughin, I.; Das, S.B.; Flowers, G.E.; Behn, M.D.; Alley, R.B.; King, M.A.; Smith, B.E.; Bamber, J.L.; Van Den Broeke, M.R.; Van Angelen, J.H. Influence of ice-sheet geometry and supraglacial lakes on seasonal ice-flow variability. *Cryosphere* **2013**, *7*, 1185–1192. [[CrossRef](#)]
23. Moon, T.; Joughin, I.; Smith, B.; Broeke, M.R.; Berg, W.J.; Noël, B.; Usher, M. Distinct patterns of seasonal Greenland glacier velocity. *Geophys. Res. Lett.* **2014**, *41*, 7209–7216. [[CrossRef](#)] [[PubMed](#)]
24. Sole, A.J.; Mair, D.W.F.; Nienow, P.W.; Bartholomew, I.D.; King, M.A.; Burke, M.J.; Joughin, I. Seasonal speedup of a Greenland marine-terminating outlet glacier forced by surface melt-induced changes in subglacial hydrology. *J. Geophys. Res. Earth Surf.* **2011**, *116*, 1–11. [[CrossRef](#)]
25. Bartholomew, I.D.; Nienow, P.; Sole, A.; Mair, D.; Cowton, T.; King, M.A. Short-term variability in Greenland Ice Sheet motion forced by time-varying meltwater drainage: Implications for the relationship between subglacial drainage system behavior and ice velocity. *J. Geophys. Res. Earth Surf.* **2012**, *117*, 1–17. [[CrossRef](#)]
26. Van de Wal, R.S.W.; Smeets, C.J.P.P.; Boot, W.; Stoffelen, M.; Van Kampen, R.; Doyle, S.H.; Wilhelms, F.; Van Den Broeke, M.R.; Reijmer, C.H.; Oerlemans, J.; et al. Self-regulation of ice flow varies across the ablation area in south-west Greenland. *Cryosphere* **2015**, *9*, 603–611. [[CrossRef](#)]
27. Fitzpatrick, A.A.W.; Hubbard, A.; Joughin, I.; Quincey, D.J.; Van As, D.; Mikkelsen, A.P.B.; Doyle, S.H.; Hasholt, B.; Jones, G.A. Ice flow dynamics and surface meltwater flux at a land-terminating sector of the Greenland ice sheet. *J. Glaciol.* **2013**, *59*, 687–696. [[CrossRef](#)]
28. Lucchitta, B.K.; Ferguson, H.M. Antarctica: Measuring glacier velocity from satellite images. *Science* **1986**, *234*, 1105–1108. [[CrossRef](#)] [[PubMed](#)]
29. Dehecq, A.; Gourmelen, N.; Trouve, E. Deriving large-scale glacier velocities from a complete satellite archive: Application to the Pamir-Karakoram-Himalaya. *Remote Sens. Environ.* **2015**, *162*, 55–66. [[CrossRef](#)]
30. Fahnestock, M.; Scambos, T.; Moon, T.; Gardner, A.; Haran, T.; Klinger, M. Rapid large-area mapping of ice flow using Landsat 8. *Remote Sens. Environ.* **2016**, *185*, 84–94. [[CrossRef](#)]
31. Armstrong, W.H.; Anderson, R.S.; Fahnestock, M.A. Spatial Patterns of Summer Speedup on South Central Alaska Glaciers. *Geophys. Res. Lett.* **2017**, *44*, 9379–9388. [[CrossRef](#)]
32. Gardner, A.S.; Moholdt, G.; Scambos, T.; Fahnestock, M.; Ligtenberg, S.; Van Den Broeke, M.; Nilsson, J. Increased West Antarctic ice discharge and East Antarctic stability over the last seven years. *Cryosphere* **2018**, *12*, 521–547. [[CrossRef](#)]

33. Joughin, I.; Winebrenner, D.P.; Fahnestock, M.A. Observations of ice-sheet motion in Greenland using satellite radar interferometry. *Geophys. Res. Lett.* **1995**, *22*, 571–574. [[CrossRef](#)]
34. Lucchitta, B.K.; Rosanova, C.E.; Mullins, K.F. Velocities of Pine Island Glacier, West Antarctica, from ERS-1 SAR images. *Ann. Glaciol.* **1995**, *21*, 277–283. [[CrossRef](#)]
35. Goldstein, R.M.; Engelhardt, H.; Kamb, B.; Frolich, R.M. Satellite Radar Interferometry for Monitoring Ice Sheet Motion: Application to an Antarctic Ice Stream. *Science* **1993**, *262*, 1525–1530. [[CrossRef](#)] [[PubMed](#)]
36. Rignot, E.; Velicogna, I.; Van Den Broeke, M.R.; Monaghan, A.; Lenaerts, J.T.M. Acceleration of the contribution of the Greenland and Antarctic ice sheets to sea level rise. *Geophys. Res. Lett.* **2011**, *38*, 1–5. [[CrossRef](#)]
37. Joughin, I.; Smith, B.E.; Howat, I.M.; Scambos, T.; Moon, T. Greenland flow variability from ice-sheet-wide velocity mapping. *J. Glaciol.* **2010**, *56*, 415–430. [[CrossRef](#)]
38. Nagler, T.; Rott, H.; Hetzenecker, M.; Wuite, J.; Potin, P. The Sentinel-1 Mission: New Opportunities for Ice Sheet Observations. *Remote Sens.* **2015**, *7*, 9371–9389. [[CrossRef](#)]
39. Joughin, I.; Smith, B.E.; Howat, I. Greenland Ice Mapping Project: Ice Flow Velocity Variation at sub-monthly to decadal time scales. *Cryosphere* **2018**, *12*, 2211–2227. [[CrossRef](#)]
40. Lemos, A.; Shepherd, A.; Mcmillan, M.; Hogg, A.E.; Hatton, E.; Joughin, I. Ice velocity of Jakobshavn Isbræ, Petermann Glacier, Nioghalvfjærdsfjorden and Zachariæ Isstrøm, 2015–2017, from Sentinel 1-a/b SAR imagery. *Cryosphere* **2018**, *12*, 2087–2097. [[CrossRef](#)]
41. Bartholomew, I.D.; Nienow, P.; Sole, A.; Mair, D.; Cowton, T.; King, M.A.; Palmer, S. Seasonal variations in Greenland Ice Sheet motion: Inland extent and behaviour at higher elevations. *Earth Planet. Sci. Lett.* **2011**, *307*, 271–278. [[CrossRef](#)]
42. Sole, A.; Nienow, P.W.; Bartholomew, I.D.; Mair, D.W.F.; Cowton, T.R.; Tedstone, A.J.; King, M.A. Winter motion mediates dynamic response of the Greenland Ice Sheet to warmer summers. *Geophys. Res. Lett.* **2013**, *40*, 3940–3944. [[CrossRef](#)]
43. Chandler, D.M.; Wadham, J.L.; Lis, G.P.; Cowton, T.; Sole, A.; Bartholomew, I.D.; Telling, J.; Nienow, P.; Bagshaw, E.B.; Mair, D.; et al. Evolution of the subglacial drainage system beneath the Greenland Ice Sheet revealed by tracers. *Nat. Geosci.* **2013**, *6*, 195–198. [[CrossRef](#)]
44. Howat, I.M.; de la Peña, S.; van Angelen, J.H.; Lenaerts, J.T.M.; van den Broeke, M.R. Brief Communication: “Expansion of meltwater lakes on the Greenland Ice Sheet”. *Cryosphere* **2013**, *7*, 201–204. [[CrossRef](#)]
45. Leeson, A.A.; Shepherd, A.; Palmer, S.; Sundal, A.; Fettweis, X. Simulating the growth of supraglacial lakes at the western margin of the Greenland ice sheet. *Cryosphere* **2012**, *6*, 1077–1086. [[CrossRef](#)]
46. Leeson, A.A.; Shepherd, A.; Sundal, A.V.; Johansson, A.M.; Selmes, N.; Briggs, K.; Hogg, A.E.; Fettweis, X. A comparison of supraglacial lake observations derived from MODIS imagery at the western margin of the Greenland ice sheet. *J. Glaciol.* **2013**, *59*, 1179–1188. [[CrossRef](#)]
47. Leeson, A.; Shepherd, A.; Briggs, K.; Fettweis, X. Supraglacial lakes on Greenland migrate inland under warming climate. *Nat. Clim. Chang.* **2015**, *16*, 51–55. [[CrossRef](#)]
48. Clason, C.C.; Mair, D.W.F.; Nienow, P.W.; Bartholomew, I.D.; Sole, A.; Palmer, S.; Schwanghart, W. Modelling the transfer of supraglacial meltwater to the bed of Leverett Glacier, Southwest Greenland. *Cryosphere* **2015**, *9*, 123–138. [[CrossRef](#)]
49. Koziol, C.P.; Arnold, N. Modelling seasonal meltwater forcing of the velocity of land-terminating margins of the Greenland Ice Sheet. *Cryosphere* **2018**, *12*, 971–991. [[CrossRef](#)]
50. GAMMA REMOTE SENSING. Sentinel-1 Processing with GAMMA Software. Version 1.2; GAMMA Remote Sensing AG: Gumligen, Switzerland, 2015.
51. Strozzi, T.; Luckman, A.; Murray, T.; Wegmuller, U.; Werner, C.L. Glacier motion estimation using SAR offset-tracking procedures. *IEEE Trans. Geosci. Remote Sens.* **2002**, *40*, 2384–2391. [[CrossRef](#)]
52. Pritchard, H.; Murray, T.; Luckman, A.; Strozzi, T.; Barr, S. Glacier surge dynamics of Sortebrae, east Greenland, from synthetic aperture radar feature tracking. *J. Geophys. Res.* **2005**, *110*, 1–13. [[CrossRef](#)]
53. Paul, F.; Bolch, T.; Käab, A.; Nagler, T.; Nuth, C.; Scharrer, K.; Shepherd, A.; Strozzi, T.; Ticconi, F.; Bhambri, R.; et al. The glaciers climate change initiative: Methods for creating glacier area, elevation change and velocity products. *Remote Sens. Environ.* **2015**, *162*, 408–426. [[CrossRef](#)]
54. Howat, I.M.; Negrete, A.; Smith, B.E. The Greenland Ice Mapping Project (GIMP) land classification and surface elevation data sets. *Cryosphere* **2014**, *8*, 1509–1518. [[CrossRef](#)]

55. Hogg, A.E.; Shepherd, A.; Cornford, S.L.; Briggs, K.H.; Gourmelen, N.; Graham, J.; Joughin, I.; Mouginot, J.; Nagler, T.; Payne, A.J.; et al. Increased ice flow in Western Palmer Land linked to ocean melting. *Geophys. Res. Lett.* **2017**, *1–9*. [[CrossRef](#)]
56. Liao, H.; Meyer, F.J.; Scheuchl, B.; Mouginot, J.; Joughin, I.; Rignot, E. Ionospheric correction of InSAR data for accurate ice velocity measurement at polar regions. *Remote Sens. Environ.* **2018**, *209*, 166–180. [[CrossRef](#)]
57. De Lange, R.; Luckman, A.; Murray, T. Improvement of satellite radar feature tracking for ice velocity derivation by spatial frequency filtering. *IEEE Trans. Geosci. Remote Sens.* **2007**, *45*, 2309–2318. [[CrossRef](#)]
58. Morlighem, M.; Williams, C.; Rignot, E.; An, L.; Arndt, J.E.; Bamber, J.; Catania, G.; Chauché, N.; Dowdeswell, J.A.; Dorschel, B.; et al. Zinglersen IceBridge BedMachine Greenland. NASA National Snow and Ice Data Center Distributed Active Archive Center; Version 3; Boulder, Colorado, USA, 2017. [[CrossRef](#)]
59. Ryser, C.; Lüthi, M.P.; Andrews, L.C.; Hoffman, M.J.; Catania, G.A.; Hawley, R.L.; Neumann, T.A.; Kristensen, S.S. Sustained high basal motion of the Greenland ice sheet revealed by borehole deformation. *J. Glaciol.* **2014**, *60*, 647–660. [[CrossRef](#)]
60. Armstrong, W.H.; Anderson, R.S.; Allen, J.; Rajaram, H. Modeling the WorldView-derived seasonal velocity evolution of Kennicott Glacier, Alaska. *J. Glaciol.* **2016**, *62*, 763–777. [[CrossRef](#)]
61. Hewitt, I.J. Seasonal changes in ice sheet motion due to melt water lubrication. *Earth Planet. Sci. Lett.* **2013**, *371–372*, 16–25. [[CrossRef](#)]



© 2018 by the authors. Licensee MDPI, Basel, Switzerland. This article is an open access article distributed under the terms and conditions of the Creative Commons Attribution (CC BY) license (<http://creativecommons.org/licenses/by/4.0/>).